

Some Statistical Physics Approaches for Trends and Predictions in Meteorology

Kristinka Ivanova¹, Marcel Ausloos², Thomas Ackerman³, Hampton Shirer¹, and Eugene Clothiaux¹

¹ Pennsylvania State University, University Park PA 16802, USA

² SUPRAS & GRASP, B5, University of Liège, B-4000 Liège, Belgium

³ Pacific Northwest National Laboratory, Richland, WA 99352, USA

Summary. Specific aspects of time series analysis are discussed. They are related to the analysis of atmospheric data that are pertinent to clouds. A brief introduction on some of the most interesting topics of current research on climate/weather predictions is given. Scaling properties of the liquid water path in stratus clouds are analyzed to demonstrate the application of several methods of statistical physics for analyzing data in atmospheric sciences, and more generally in geophysics. The breaking up of a stratus cloud is shown to be related to changes in the type of correlations in the fluctuations of the signal that represents the total vertical amount of liquid water in the stratus cloud. It is demonstrated that the correlations of the liquid water path fluctuations exist indeed in a more complex way than usually known through their multi-affine dependence.

1 Introduction

Earth's climate is determined by complex interactions between sun, oceans, atmosphere, land and biosphere [1,2]. The composition of the atmosphere is particularly important because certain gases, including water vapor, carbon dioxide, etc., absorb heat radiated from the Earth's surface. As the atmosphere warms, it in turn radiates heat back to the surface that increases the earth's mean surface temperature by some 30 K above the value that would occur in the absence of a radiation-trapping atmosphere [1]. Perturbations in the concentration of these radiatively active gases alter the intensity of this effect on the earth's climate.

Climate change, a major concern of everyone, is a focus of current atmospheric research. Understanding the processes and properties that effect atmospheric radiation and, in particular, the influence of clouds and the role of cloud radiative feedback, are issues of scientific interest. This leads to efforts to improve not only models of the earth's climate but also predictions of climate change [3,4], whence weather prediction and climate models.

Lorenz's [5] famous pioneering work on chaotic systems using a simple set of nonlinear differential equations was motivated by considerations of weather prediction. However, predicting the results of complex nonlinear interactions that are taking place in an open system is a difficult task. Yet physicists have

only the Navier-Stokes equations [6] at hand for describing fluid motion, in terms of such quantities as mass, pressure, temperature, humidity, velocity, energy exchange, ... whence for describing the variety of processes that take place in the atmosphere. Since controlled experiments cannot be performed on the climate system, we rely on use of models to identify cause-and-effect relationships. It is also essential to concentrate on predicting the uncertainty in forecast models of weather and climate [7,8].

Modeling the impact of clouds is difficult because of their complex and differing effects on weather and climate. Clouds can reflect incoming sunlight and, therefore, contribute to cooling, but they also absorb infrared radiation leaving the earth and contribute to warming. High cirrus clouds, for example, may have the impact of warming the atmosphere. Low-lying stratus clouds, which are frequently found over oceans, can contribute to cooling. In order to successfully model and predict climate, we must be able to both describe the effect of clouds in the current climate and predict the complex chain of events that might modify the distribution and properties of clouds in an altered climate.

Much attention has been paid recently [9] to the importance of the main substance of the atmosphere and clouds, water in its three forms — vapor, liquid and solid, for buffering the global temperature against reduced or increased solar heating [10]. Owing to its special properties, it is believed, that water establishes lower and upper boundaries on how far the temperature can drift from current values.

The role of clouds and water vapor in climate change is not well understood; yet water vapor is the most abundant greenhouse gas and directly affects cloud cover and the propagation of radiant energy. In fact, there may be positive feedback between water vapor and other greenhouse gases. Carbon dioxide and other gases from human activities slightly warm the atmosphere, increasing its ability to hold water vapor. Increased water vapor can amplify the effect of an incremental increase of other greenhouse gases.

Other studies suggest that the heliosphere influences the climate on Earth via global mechanism that affects cloud cover [11,12]. Surprisingly the influence of solar variability is found to be strongest in low clouds (3 km), which points to a microphysical mechanism involving aerosol formation that is enhanced by ionization due to cosmic rays.

Beyond the scientifically sound and highly sophisticated computer models, there is still space for simple approaches, based on standard statistical physics techniques and ideas, in particular based on the scaling hypothesis [13], phase transitions [14] and percolation theory aspects [15]. Analogies can be found between meteorological and other phenomena in social or natural science [16]. However to distinguish cases and patterns due to "external field" influences or self-organized criticality [17] is not obvious indeed. The coupling between human activities and deterministic physics is hard to model on simple terms.

There have been several reports that long-range power-law correlations can be extracted from apparently stochastic time series in meteorology [18,19] and multi-affine properties [20,21] can be identified related to atmospheric turbulence [22]. The same type of investigations has already appeared and seems promising in atmospheric science. In the following we touch upon a brief review of some statistical physics approaches for testing scaling hypothesis in meteorology and for identifying the self-affine or multi-affine nature of atmospheric quantities. We apply useful numerical statistical techniques on real time data measurements; for illustration we have selected stratus clouds.

Restricting ourselves to cloud physics and fractal geometry ideas, leads to many questions, such as on the perimeter-area relationship of rain and cloud areas [23], the fractal dimension of their shape or ground projection [24] or modelization of fractally homogeneous turbulence [25]. The cloud inner structure, content, temperature, life time and effects on ground level phenomena or features are of constant interest and prone to physical modelisation [26]. Recently, we reported about long-range power-law correlations [27,28] and multi-affine properties [29] of stratus cloud liquid water fluctuations.

1.1 Techniques of time series analysis

The variety of systems that apparently display scaling properties ranges from base-pair correlations in DNA and inter-beat intervals of the human heart, to large, spatially extended geophysical processes, such as earthquakes, and signals produced by complex systems, such as financial indices in economics. The current paradigm is that these systems obey “universal” laws due to the underlying nonlinear dynamics and are independent of the microscopic details. Therefore one can consider in meteorology to obtain characteristic quantities using the same modern statistical physics methods as done in all of the other cases. Whence we will focus on several techniques to describe the scaling properties of meteorological time series, like the Fourier power spectrum of the signal [30], detrended fluctuation analysis (DFA) method [31] and its extension local DFA method [27], and multi-affine and singularity analysis [29,32]. One can go beyond these methods using wavelet techniques [33] or Zipf diagrams [34,35,36]. The Fokker-Planck equation [37] for describing the liquid water path [38], which is studied here below, is also of interest.

2 Experimental techniques and data acquisition

Quantitative observations of the atmosphere are made in many different ways. Experimental/observational techniques to study the atmosphere rely on physical principles. One important type of observational techniques is that of *remote sensing*, which depends on the detection of electromagnetic radiation emitted, scattered or transmitted by the atmosphere. The instruments can be placed at aircrafts, on balloons or on the ground. Remote-sensing techniques can be divided into *passive* and *active* types. In passive remote sensing,

the radiation measured is of natural origin, for example the thermal radiation emitted by the atmosphere, or solar radiation transmitted or scattered by the atmosphere. Most space-born remote sensing methods are passive. In active remote sensing, a transmitter, e.g. a radar, is used to direct pulses of radiation into the atmosphere, where they are scattered by atmospheric molecules, aerosols or inhomogeneities in the atmospheric structure. Some of the scattered radiation is then detected by some receiver. Each of these techniques has its advantages and disadvantages. Remote sensing from satellites can give near-global coverage, but can provide only averaged values of the measured quantity over large regions, of order of hundreds of kilometers in horizontal extent and several kilometers in the vertical direction. Satellite instruments are expensive to put into orbit and cannot usually be repaired if they fail. Ground-based radars can provide data with very high vertical resolution (by measuring small differences in the time delays of the return pulses), but only above the radar site.

For illustrative purposes, we will use microwave radiometer data obtained from the Department of Energy (DOE) Atmospheric Radiation Measurement (ARM) program [39] site located at the Southern Great Plains (SGP) central facility [40]. For detailed presentation of other remote sensing techniques the reader can consult Andrews [1] and/or Rees [41].

In this study we focus on stratus cloud data. For comparison the cumulus cloud scale is too small to be represented individually in today's numerical models [42]. Due to their relatively small sizes cumulus clouds produce short time series when remote sensing measurements are applied. Therefore they are not particularly suitable for the techniques that are outlined in this report. However their role in the transport of heat, moisture and momentum must be considered in numerical models.

The data used in this study are the vertical column amounts of cloud liquid water that are retrieved from the radiances, recorded as brightness temperatures, measured with a Radiometrics Model WVR-1100 microwave radiometer at frequencies of 23.8 and 31.4 GHz [43,44,45]. The microwave radiometer is equipped with a Gaussian-lensed microwave antenna whose small-angle receiving cone is steered with a rotating flat mirror [40]. The microwave radiometer is located at the DOE ARM program SGP central facility and is operated in the vertically pointing mode. In this mode the radiometer makes sequential 1 s radiance measurements in each of the two channels while pointing vertically upward into the atmosphere. After collecting these radiances the radiometer mirror is rotated to view a blackbody reference target. For each of the two channels the radiometer records the radiance from the reference immediately followed by a measurement of a combined radiance from the reference and a calibrated noise diode. This measurement cycle is repeated once every 20 s.

A shorter measurement cycle does not necessarily lead to a larger number of independent samples. For example, clouds at 2 km altitude moving at 10

ms^{-1} take 15 s to advect through a radiometer field-of-view of approximately 5° . Note that the 1 s sky radiance integration time ensures that the retrieved quantities correspond to a specific column of cloud above the instrument, as opposed to some longer time average of the cloud properties in the column above the instrument. The field of view of the microwave radiometer is 5.7° at 23.8 GHz and 4.6° at 31.4 GHz.

Based on a standard model [43,45] (see Appendix), the microwave radiometer measurements at the two frequency channels of 23.8 and 31.4 GHz are used to obtain time series of liquid water path (LWP) that corresponds to the total amount of liquid water within the vertical column of the atmosphere that has been remotely sounded. The error for the liquid water retrieval is estimated to be less than about 0.005 g/cm^2 [45].

The liquid water path (LWP) data $y(t)$ considered in this study are obtained on April 3-5, 1998 and are shown in Fig. 1a.

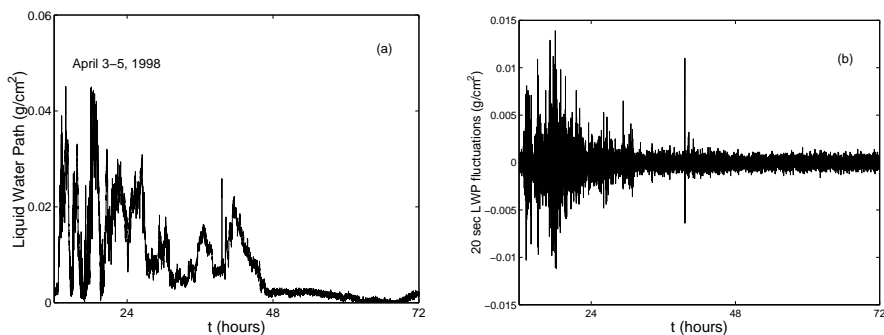


Fig. 1. (a) Time dependence of liquid water path as obtained at the ARM Southern Great Plains site with time resolution of 20 s during the period from April 3 to 5, 1998. The time series contains $N = 10740$ data points. On x-axis $t=24$ h marks midnight on April 3, $t=48$ h corresponds to midnight on April 4 and $t=72$ h corresponds to midnight on April 5, 1998. (b) Small-scale gradient field of the LWP signal, e.g. fluctuations of LWP for a time interval equal to the discretization step of the measurements.

3 Nonstationarity and Spectral density

Fluctuations of the LWP signal $y(t)$ (data in Fig. 1a) are plotted in Fig. 1b for the time interval equal to the discretization step of the data, i.e. $\Delta t = 20$ sec. This time series is also called the small-scale gradient field. Other values of time intervals to study fluctuations of a signal can be of interest to search for changes in the type and strength of the correlations [46]. This approach will not be pursued here.

One approach to test the type of the LWP fluctuations is to estimate the nonstationarity of the signal. The power spectral density $S(f)$ of the time series $y(t)$ is defined as the Fourier transform of the signal. For supposedly self-affine signals $S(f)$ is expected to follow a power-law dependence in terms of the frequency f ,

$$S(f) \sim f^{-\beta}. \quad (1)$$

Equation (1) allows one to put the phenomena that produce the time series into the class of *self-affine* phenomena.

It has been argued [47,48] that the spectral exponent β contains information about the degree of stationarity of the signal $y(t)$. Depending on the value of β the time series is called stationary or not; for $\beta < 1$, the signal is statistically invariant by transition in time, thus called stationary. If $\beta > 1$, the signal is nonstationary. In addition, if $\beta < 3$ the increments of the signal form a stationary series, in particular the small-scale gradient field is stationary. Many geophysical fields are nonstationary with stationary increments ($1 < \beta < 3$) over some scaling range. The upper bound of the nonstationary regime is required to keep the field values within their physically accessible range by limiting the amplitude of the large scale fluctuations, which corresponds to a flatter part of the spectrum at low frequencies.

Brownian motion is characterized by $\beta = 2$, and white noise by $\beta = 0$. Indeed the Brownian motion or random walk $z(x)$ is a classical example of a nonstationary process. We know that its variance $\langle z^2(x) \rangle$ is proportional to x , which proves the nonstationarity in the one-point statistics. However, in the framework of two-point statistics, this result has a different interpretation. The variance of the ‘‘increment’’ $z(x + \xi) - z(x)$ increases linearly with ξ , independently of x , which is an indication of the stationarity of the increments.

The range over which the β exponent is well defined in Eq. (1) indicates the range over which the scaling properties of the time series are invariant. The power spectral density $S(f)$ of the liquid water path data measured on April 3-4, 1998 is shown in Fig. 2. The spectral exponent $\beta = 1.56 \pm 0.03$ indicates a nonstationary time series.

4 Roughness and Detrended Fluctuation Analysis

The fractal dimension [13,49,50,51] D is often used to characterize the roughness of profiles [52]. Several methods are used for measuring D , like the box counting method, though not quite efficient; many others are found in the literature as seen in [13,49,50,51] and here below. For topologically one dimensional systems, the fractal dimension D is related to the exponent β by

$$\beta = 5 - 2D. \quad (2)$$

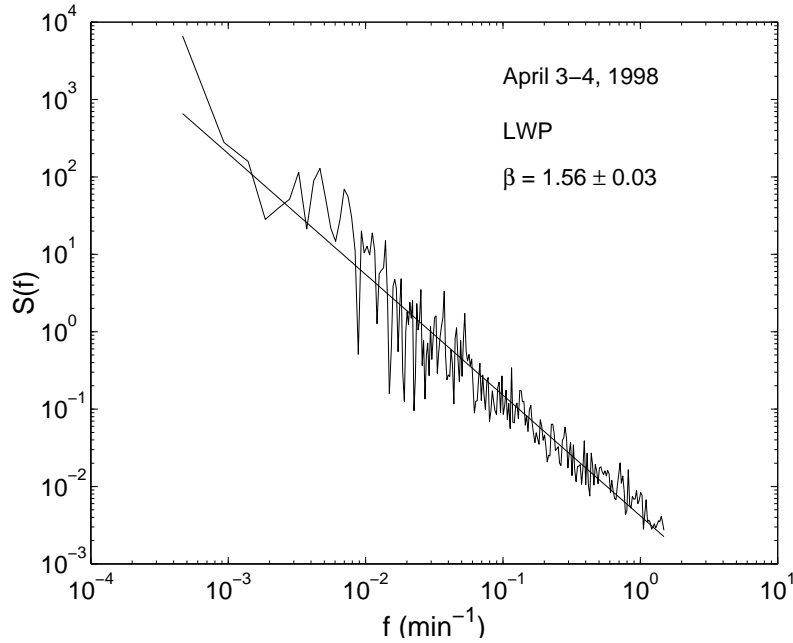


Fig. 2. Power spectral density for data measured on April 3-4, 1998.

Another "measure" of the signal roughness is sometimes given by the Hurst Hu exponent, first defined in the "rescale range theory" (of Hurst [53,54]) who suggested a method to estimate the persistence of the Nile floods and droughts. The Hurst method consists of listing the differences between the observed value at a discrete time t over an interval with size N in which the mean has been taken. The upper (y_M) and lower (y_m) values in that interval define the range $R_N = y_M - y_m$. The root mean square deviation S_N being also calculated, the "rescaled range" is R_N/S_N is expected to behave like N^{Hu} . This means that for a (discrete) self-affine signal $y(t)$, the neighborhood of a particular point on the signal can be rescaled by a factor b using the roughness (or Hurst [49,50]) exponent Hu and defining the new signal $b^{-Hu}y(bt)$. For the exponent value Hu , the frequency dependence of the signal so obtained should be undistinguishable from the original one, i.e. $y(t)$.

The roughness (Hurst) exponent Hu can be calculated from the height-height correlation function $c_1(\tau)$ or first order structure function that supposed to behave like

$$c_1(\tau) = \langle |y(t_{i+r}) - y(t_i)| \rangle_\tau \sim \tau^{H_1} \quad (3)$$

whereas

$$Hu = 1 + H_1, \quad (4)$$

rather than from the box counting method. For a *persistent* signal, $H_1 > 1/2$; for an *anti-persistent* signal, $H_1 < 1/2$. Flandrin has theoretically proved [55] that

$$\beta = 2Hu - 1, \quad (5)$$

thus $\beta = 1 + 2H_1$. This implies that the classical random walk (Brownian motion) is such that $Hu = 3/2$. It is clear that

$$D = 3 - Hu. \quad (6)$$

Fractional Brownian motion values in other fields [56,57,58] are practically found to lie between 1 and 2. Since a white noise is a truly random process, it can be concluded that $Hu = 1.5$ implies an uncorrelated time series [51].

Thus $D > 1.5$, or $Hu < 1.5$ implies antipersistence and $D < 1.5$, or $Hu > 1.5$ implies persistence. From preimposed Hu values of a fractional Brownian motion series, it is found that the equality here above usually holds true in a very limited range and β only slowly converges toward the value Hu [30,59].

The above exponents and parameters can be obtained within the detrended fluctuations analysis (DFA) method [31]. The DFA method is a tool used for sorting out correlations in a self-affine time series with stationary increments [58,60,61]. It provides a simple quantitative parameter - the scaling exponent α , which is a signature of the correlation properties of the signal. The advantages of DFA over many methods are that it permits detection of long-range correlations embedded in seemingly non-stationary time series, and also that inherent trends are avoided at all time scales. The DFA technique consists in dividing a time series $y(t)$ of length N into N/τ nonoverlapping boxes (called also windows), each containing τ points [31]. The local trend $z(n)$ in each box is defined to be the ordinate of a linear least-square fit of the data points in that box. The detrended fluctuation function $F^2(\tau)$ is then calculated following:

$$F^2(\tau) = \frac{1}{\tau} \sum_{n=k\tau+1}^{(k+1)\tau} [y(n) - z(n)]^2 \quad k = 0, 1, 2, \dots, \left(\frac{N}{\tau} - 1\right) \quad (7)$$

Averaging $F^2(\tau)$ over the N/τ intervals gives the mean-square fluctuations

$$\langle F^2(\tau) \rangle^{1/2} \sim \tau^\alpha. \quad (8)$$

The DFA exponent α is obtained from the power law scaling of the function $\langle F^2(\tau) \rangle^{1/2}$ with τ , and represents the correlation properties of the signal: $\alpha = 1/2$ indicates that the changes in the values of a time series are random and, therefore, uncorrelated with each other. If $\alpha < 1/2$ the signal is

anti-persistent (anti-correlated), while $\alpha > 1/2$ indicate positive persistency (correlation) in the signal.

Results of the DFA analysis of liquid water path data measured on April 3-4, 1998 are plotted in Fig. 3a. The DFA function is close to a power law with an exponent $\alpha = 0.34 \pm 0.01$ holding from 3 to 60 minutes. This scaling range is somewhat shorter than the 150 min scaling range we obtained [28] for a stratus cloud during the period Jan. 9-14, 1998 at the ARM SGP site. A crossover to $\alpha = 0.50 \pm 0.01$ is readily seen for longer correlation times [61] to about 2 h, after which the statistics of the DFA function is not reliable. One should note that for cloud data the lower limit of the scaling range is determined by the resolution and discretization steps of the measurements. Since such clouds move at an average speed of *ca.* 10 m/s and the instrument is always directed toward the same point of the atmosphere, the 20s discretization step is chosen to ensure ergodic sampling for an about 5° observation angle of the instrument. The upper scaling range limit depends on the cloud life time.

The value of $\alpha \approx 0.3$ can be interpreted as the H_1 parameter of the multifractal analysis of liquid water content [32] and of liquid water path [29]. The existence of a crossover suggests two types of correlated events as in classical fracture processes: (i) On one hand, the nucleation part and the growth of diluted droplets occur in "more gas-like regions". This process is typically slow and is governed by long range Brownian-like fluctuations; it is expected to follow an Eden model-like [62] growth, with a trivial scaling exponent, as $\alpha = 0.5$ (Fig. 3b); (ii) The faster processes with more Levy-like fluctuations are those which link together various fracturing parts of the cloud, and are necessarily antipersistent as long as the cloud remains thermodynamically stable; they occur at shorter correlation times, and govern the cloud breaking final regime as in any percolation process [14], - with an intrinsic non-trivial scaling exponent ~ 0.3 .

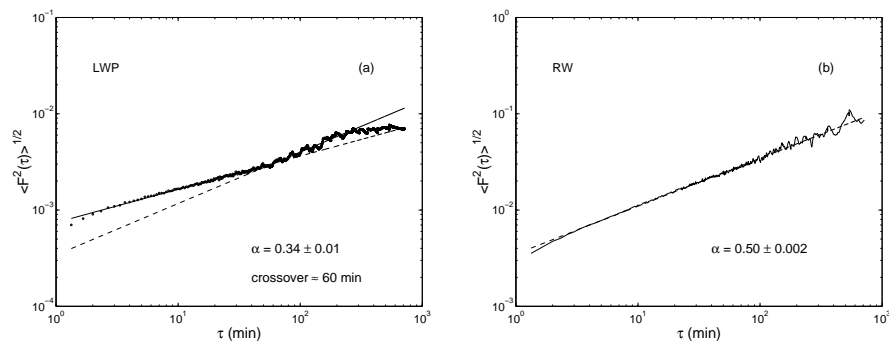


Fig. 3. (a) Detrended fluctuation function $\langle F^2(\tau) \rangle^{1/2}$ for data measured on April 3-4, 1998. (b) DFA-function for Brownian walk signal scales with $\alpha = 0.50 \pm 0.01$ and is plotted for comparison.

Several remarks are in order. Recently a rigorous relation between detrended fluctuation analysis and power spectral density analysis for stochastic processes is established [64]. Thus, if the two scaling exponents α and β are well defined, $\beta = 2\alpha + 1$ holds for $0 < \alpha < 1$ ($1 < \beta < 3$) for fractional Brownian walks [59,63], establishing the relation between detrended fluctuation analysis and power spectral density analysis for stochastic processes

In terms of the exponents (α and β) of the signal, we can talk about pink noise $\alpha = 0$ ($\beta = 1$), brown noise $\alpha = 1/2$ ($\beta = 2$) or black noise $\alpha > 1/2$ ($\beta > 2$) [13]. Black noise is related to persistence. In contrast, inertial subrange turbulence for which $\beta = 5/3$ gives $\alpha = 1/3$ [65], which places it in the antipersistence regime.

The two scaling exponents α and β for the liquid water path signal are only approximately close to fulfilling the relation $\beta = 2\alpha + 1$. This can be interpreted to be due to the peculiarities of the spectral method [66]. In general, the Fourier transform is inadequate for non-stationary signals. Also it is sensitive to possible trends in the data. There are different techniques suggested to correct these deficiencies of the spectral method [67,68], like detrending the data before taking the Fourier transform. However, this may lead to questions about the accuracy of the spectral exponent [69].

5 Time dependence of the correlations

In previous section we study the type of correlations that exist in the liquid water path signal measured during cloudy atmospheric conditions, on April 3-4, 1998. Here we focus on the evolution of these correlations during the same time interval but also continuing on the next day, April 5, when the stratus cloud disappears. In doing so we can further study the influence of the time lag on correlations in the signal.

In order to probe the existence of so called *locally correlated* and *decorrelated* sequences [58], one can construct a so-called observation box with a certain width, τ , place the box at the beginning of the data, calculate α for the data in that box, move the box by $\Delta\tau$ toward the right along the signal sequence, calculate α in that box, a.s.o. up to the N -th point of the available data. A time dependent α exponent may be expected.

We apply this technique to the liquid water path data signal and the result is shown in Fig. 4. For this illustration we have chosen two window sizes, i.e. 4 h and 6 h, moving the window with a step of $\Delta\tau = 1$ h. Since the value of *local* α can only be known after all data points are taken into account in a box, the reported value corresponds to that at the upper most time value for that given box in Fig. 4. One clearly observes that the α exponent value does not vary much when the value of τ and $\Delta\tau$ are changed. As could be expected there is more roughness if the box is narrower. The local α exponent value is always significantly below $1/2$. By analogy with

financial and biological studies, this is interpreted as a phenomenon related to the *fractional Brownian motion* process mentioned above.

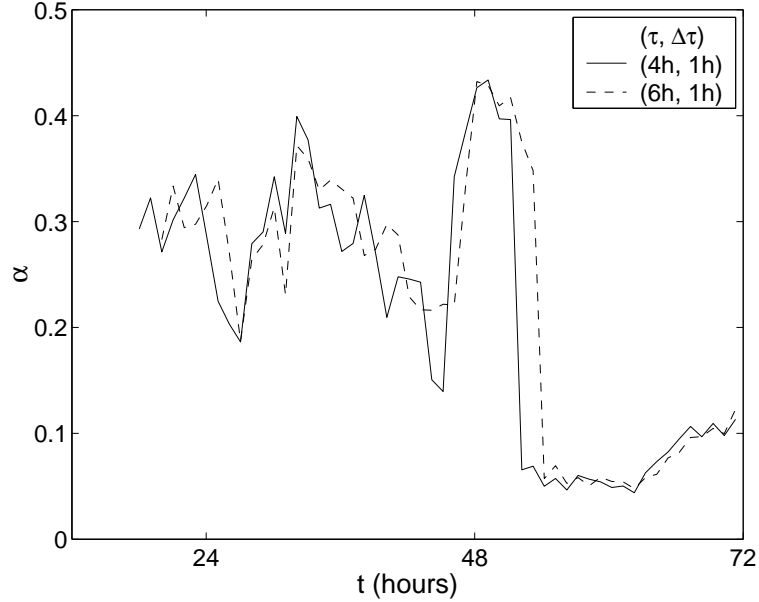


Fig. 4. Local α -exponent from DFA analysis for data in Fig. 1a.

The results from this local DFA analysis applied to LWP data (Fig. 4) indicate two well defined regions of scaling with different values of α . The first region corresponds to the first two days when a thick stratus cloud existed. The average value of the local scaling exponent over this period is $\alpha = 0.34 \pm 0.01$; it is followed by a sharp rise to 0.5, then by a sharp drop below $\alpha = 0.1$ when there is a clear sky day. These values of local α are well defined for a scaling time (range) interval extending between 2 and 25 minutes for the various τ and $\Delta\tau$ combinations. The value of α , close to 0.3, indicates a very large antipersistence, thus a set of fluctuations tending to induce a great stability of the system and great antipersistence of the prevailing meteorology, - in contrast to the case in which there would be a persistence of the system which would be dragged out of equilibrium; it would equally imply good predictability. This implies that specific fluctuation correlation dynamics could be usefully inserted as ingredients in *ad hoc* models.

The appearance of a patch of clouds and clear sky following a period of thick stratus can be interpreted as a non equilibrium transition. The $\alpha = 1/2$ value in financial fluctuations [58] was observed to indicate a period of relative economic calm. The appropriately called thunderstorm of activities and other bubble explosions in the financial field correspond to a value different from

1/2 [70]. Thus we emphasize here that stable states can occur for α values that do not correspond to the Brownian 1/2 value. We conclude that the fluctuation behavior is an observational feature more important than the peak appearance in the raw data. Moreover, from a fundamental point of view, it seems that the variations of α are as important as the value itself [58]. From the point of view of predictability, α values significantly different from 1/2 are to be preferred because such values imply a great degree of predictability and stability of the system.

6 Multi-affinity and Intermittency

The variations in the local α -exponent suggest that the nature of the correlations changes with time. As a consequence the evolution of the time series can be decomposed into successive persistent and anti-persistent sequences [58], and multi-affine behavior can be expected. Multi-affine properties of a time dependent signal $y(t)$ are described by the so-called “q-th” order structure functions

$$c_q = \langle |y(t_{i+r}) - y(t_i)|^q \rangle \quad i = 1, 2, \dots, N - r \quad (9)$$

where the average is taken over all possible pairs of points that are apart from each other a distance $\tau = y(t_{i+r}) - y(t_i)$.

Assuming a power law dependence of the structure function, the $H(q)$ spectrum is defined through the relation [71,72]

$$c_q(\tau) \sim \tau^{qH(q)} \quad q \geq 0 \quad (10)$$

The *intermittency* of the signal can be studied through the so-called singular measure analysis. The first step that this technique require is defining a basic measure $\varepsilon(1; l)$ as

$$\varepsilon(1; l) = \frac{|\Delta y(1; l)|}{\langle \Delta y(1; l) \rangle}, \quad l = 0, 1, \dots, N - 1 \quad (11)$$

where $\Delta y(1; l) = y(t_{i+1}) - y(t_i)$ is the small-scale gradient field and

$$\langle \Delta y(1; l) \rangle = \frac{1}{N} \sum_{l=0}^{N-1} |\Delta y(1; l)|. \quad (12)$$

This is indeed deriving a stationary nonnegative field from a nonstationary data and this is the simplest procedure to do so. Other techniques involve “fractional” derivatives [73] or second derivatives [74]. Also one can consider taking squares [75] rather than the absolute values but that leads to a linear relation between the exponents of these two measures. It is argued elsewhere [76] that the details of the procedure do not influence the final results of the singularity analysis.

We use a spatial/temporal average in Eq. (12) rather than an ensemble average, thus making an ergodicity assumption [77,78] that is our only recourse in empirical data analysis.

Next we define a series of ever more coarse-grained and ever shorter fields $\varepsilon(r;l)$ where $0 < l < N - r$ and $r = 1, 2, 4, \dots, N = 2^m$. Thus the average measure in the interval $[l; l+r]$ is

$$\varepsilon(r;l) = \frac{1}{r} \sum_{l'=l}^{l+r-1} \varepsilon(1;l') \quad l = 0, \dots, N - r \quad (13)$$

The scaling properties of the generating function are then searched for through the equation

$$\chi_q(\tau) = \langle \varepsilon(r;l)^q \rangle \sim \tau^{-K(q)}, \quad q \geq 0, \quad (14)$$

with $\tau = y(t_{i+r}) - y(t_i)$.

It should be noted that the intermittency of a signal is related to existence of extreme events, thus a distribution of events away from a Gaussian distribution, in the evolution of the process that has generated the data. If the tails of the distribution function follow a power law, then the scaling exponent defines the critical order value after which the statistical moments of the signal diverge [48]. Therefore it is of interest to probe the distribution of the fluctuations of a time dependent signal $y(t)$ prior investigating its intermittency. The distribution of the fluctuations of liquid water path signal measured on April 3-4, 1998 at the ARM Southern Great Plains site is shown in Fig. 5.

The frequency distribution is not Gaussian but is rather symmetrical. The tails of the distribution follow a power law

$$P(x) \sim \frac{1}{x^\mu} \quad (15)$$

with an exponent $\mu = 2.75 \pm 0.12$ away from the Gaussian $\mu = 2$ value. This scaling law gives support to the argument in favor of the existence of self-affine properties, as established in section 4 for the LWP signal, when applying the DFA method. The extreme events that form the tails of the probability distribution also characterize the intermittency of the signal. In Fig. 6 the multi-fractal properties of the LWP signal are expressed by two sets of scaling functions, the $H(q)$ hierarchy of functions describing the roughness of the signal and the $K(q)$ hierarchy of functions describing its intermittency as defined in Eq.(10) and Eq. (14) respectively. For $q = 1$, $H(1)$ is the value that is given by the DFA analysis.

7 Conclusions

Scaling properties of the liquid water path in stratus clouds have been analyzed to demonstrate the application of several methods of statistical physics

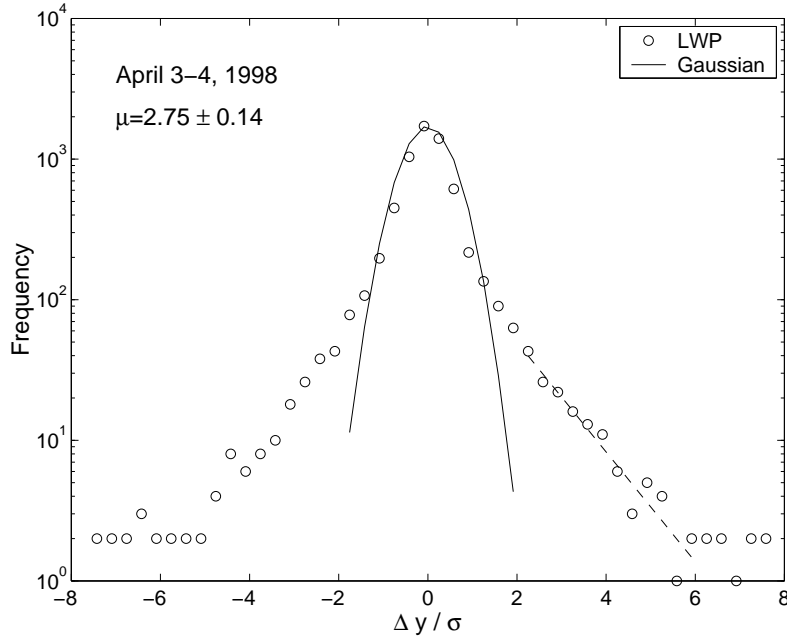


Fig. 5. Distribution of the frequency of LWP fluctuations $\Delta y / \sigma = (y(t_{i+1}) - y(t_i)) / \sigma$, where $\sigma = 0.0011 g/cm^2$ is the standard deviation of the fluctuations for LWP signal measured on April 3-4, 1998 (data in Fig. 1a)

for analyzing data in atmospheric sciences, and more generally in geophysics. We have found that the breaking up of a stratus cloud is related to changes in the type of correlations in the fluctuations of the signal, that represents the total vertical amount of liquid water in the stratus cloud. We have demonstrated that the correlations of LWP fluctuations exist indeed in a more complex way than usually known through their multi-affine dependence.

8 Acknowledgements

Thanks to Luc T. Wille for inviting us to present the above results and enticing us into writing this report. Thanks to him and the State of Florida for some financial support during the conference. This research was partially supported by Battelle grant number 327421-A-N4. We acknowledge collaboration of the U.S. Department of Energy as part of the Atmospheric Radiation Measurement Program.

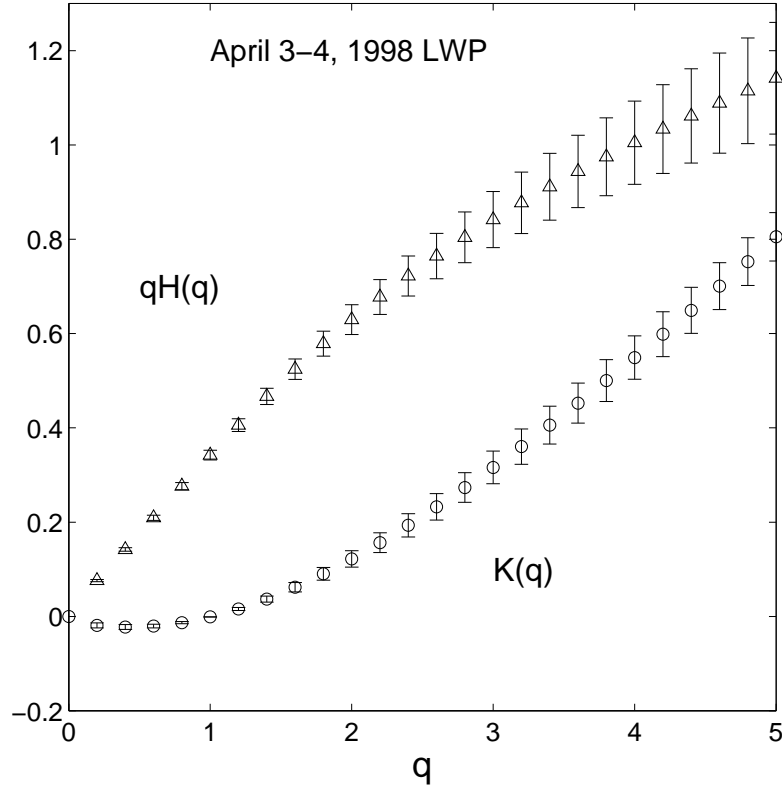


Fig. 6. The $H(q)$ and $K(q)$ functions for the LWP data obtained on April 3-4, 1998.

9 Appendix

For nonprecipitating clouds, i.e., clouds having drops sufficiently small that scattering is negligible, measurements of the microwave radiometer brightness temperature $T_{B\omega}$ can be mapped onto an opacity ν_ω parameter by

$$\nu_\omega = \ln \left[\frac{(T_{\text{mr}} - T_c)}{(T_{\text{mr}} - T_{B\omega})} \right], \quad (16)$$

where T_c is the cosmic background “big bang” brightness temperature equal to 2.8 K and T_{mr} is an estimated “mean radiating temperature” of the atmosphere.

Writing ν_ω in terms of atmospheric constituents, we have

$$\nu_\omega = \kappa_{V\omega}V + \kappa_{L\omega}L + \nu_{d\omega}, \quad (17)$$

where $\kappa_{V\omega}$ and $\kappa_{L\omega}$ are *water vapor and liquid water path-averaged* mass absorption coefficients and $\nu_{d\omega}$ is the absorption by dry atmosphere constituents (e.g., oxygen). Next, define

$$\nu_{\omega}^* = \nu_{\omega} - \nu_{d\omega} = \ln \left[\frac{(T_{mr} - T_c)}{(T_{mr} - T_{B\omega})} \right] - \nu_{d\omega}. \quad (18)$$

The 23.8 GHz channel is sensitive primarily to water vapor while the 31.4 GHz channel is sensitive primarily to cloud liquid water. Therefore two equations for the opacity can be written for each frequency and then solved for the two unknowns L and V , i.e.

$$L = l_1 \nu_{\omega_1}^* + l_2 \nu_{\omega_2}^* \quad (LWP) \quad (19)$$

and

$$V = v_1 \nu_{\omega_1}^* + v_2 \nu_{\omega_2}^*, \quad (WVP) \quad (20)$$

where

$$l_1 = - \left(\kappa_{L\omega_2} \frac{\kappa_{V\omega_1}}{\kappa_{V\omega_2}} - \kappa_{L\omega_1} \right)^{-1}, \quad (21)$$

$$l_2 = \left(\kappa_{L\omega_2} - \kappa_{L\omega_1} \frac{\kappa_{V\omega_2}}{\kappa_{V\omega_1}} \right)^{-1}, \quad (22)$$

$$v_1 = \left(\kappa_{V\omega_1} - \kappa_{V\omega_2} \frac{\kappa_{L\omega_1}}{\kappa_{L\omega_2}} \right)^{-1}, \quad (23)$$

$$v_2 = - \left(\kappa_{V\omega_1} \frac{\kappa_{L\omega_2}}{\kappa_{L\omega_1}} - \kappa_{V\omega_2} \right)^{-1}. \quad (24)$$

References

1. D. Andrews: *An Introduction to Atmospheric Physics* (Cambridge University Press, Cambridge, 2000)
2. R.A. Anshens, H.A. Panofsky, J.J. Cahir, A. Rango: *The Atmosphere* (Bell & Howell Company, Columbus, OH, 1975)
3. R.R. Rogers: *Short Course in Cloud Physics* (Pergamon Press, New York, 1976)
4. C.F. Bohren: *Clouds in a Glass of Beer* (John Wiley & Sons, New York, 1987)
5. E. N. Lorenz: *J. Atmos. Sci.* **20**, 130 (1963)
6. L. D. Landau, E.M. Lifshitz: *Fluid Mechanics* (Addison-Wesley, Reading, MA, 1959)
7. T.N. Palmer: *Phys. Rep.* **63**, 71 (2000)
8. S.G. Philander: *Phys. Rep.* **62**, 123 (1999)
9. A. Maurellis: *Physics World* **14**, 22 (2001); D. Rosenfeld, W. Woodley: *Physics World* **14**, 33 (2001)

10. H.-W. Ou: *J. Climate* **14**, 2976 (2001)
11. N.D. Marsh, H. Svensmark: *Phys. Rev. Lett.* **85**, 5004 (2000)
12. H. Svensmark: *Phys. Rev. Lett.* **81**, 5027 (1998)
13. M. Schroeder: *Fractals, Chaos and Power Laws* (W.H. Freeman and Co., New York, 1991)
14. H. E. Stanley: *Phase transitions and critical phenomena* (Oxford Univ. Press, Oxford, 1971)
15. D. Stauffer, A. Aharony: *Introduction to Percolation Theory* (Taylor & Francis, London, 1992) 2nd printing
16. P. Bak: *How Nature Works* (Springer, New York, 1996).
17. D.L. Turcotte: *Phys. Rep.* **62**, 1377 (1999)
18. E. Koscielny-Bunde, A. Bunde, S. Havlin, H. E. Roman, Y. Goldreich, H.-J. Schellnhuber: *Phys. Rev. Lett.* **81**, 729 (1998)
19. E. Koscielny-Bunde, A. Bunde, S. Havlin, Y. Goldreich: *Physica A* **231**, 393 (1993)
20. C.R. Neto, A. Zanandrea, F.M. Ramos, R.R. Rosa, M.J.A. Bolzan, L.D.A. Sa: *Physica A* **295**, 215 (2001)
21. H.F.C. Velho, R.R. Rosa, F.M. Ramos, R.A. Pielke, C.A. Degrazia, C.R. Neto, A. Zanadrea: *Physica A* **295**, 219 (2001)
22. H.A. Panofsky, J.A. Dutton: *Atmospheric turbulence* (John Wiley & Son Inc. New York 1983)
23. S. Lovejoy: *Science* **216**, 185 (1982)
24. S. Lovejoy, D. Schertzer: *Ann. Geophys. B* **4**, 401 (1986)
25. H.G.E. Hentchel, I. Procaccia: *Phys. Rev. A* **27**, 1266 (1983)
26. K. Nagel, E. Raschke: *Physica A* **182**, 519 (1992)
27. K. Ivanova, M. Ausloos: *Physica A* **274**, 349 (1999)
28. K. Ivanova, M. Ausloos, E.E. Clothiaux, T.P. Ackerman: *Europhys. Lett.* **52**, 40 (2000)
29. K. Ivanova, T. Ackerman: *Phys. Rev. E* **59**, 2778 (1999)
30. B.D. Malamud, D.L. Turcotte: *J. Stat. Plann. Infer.* **80**, 173 (1999)
31. C.-K. Peng, S.V. Buldyrev, S. Havlin, M. Simmons, H.E. Stanley A.L. Goldberger: *Phys. Rev. E* **49**, 1685 (1994)
32. A. Davis, A. Marshak, W. Wiscombe, R. Cahalan: *J. Geophys. Research.* **99**, 8055 (1994)
33. N. Decoster, S.G. Roux, A. Arneodo: *Eur. Phys. J B* **15**, 739 (2000)
34. G.K. Zipf: *Human Behavior and the Principle of Least Effort* (Addisson-Wesley, Cambridge, MA, 1949)
35. N. Vandewalle, M. Ausloos: *Physica A* **268** 240 (1999)
36. M. Ausloos, K. Ivanova: *Physica A* **270**, 526 (1999)
37. R. Friedrich, J. Peinke, Ch. Renner: *Phys. Rev. Lett.* **84**, 5224 (2000)
38. K. Ivanova, M. Ausloos, unpublished
39. G.M. Stokes, S.E. Schwartz: *Bull. Am. Meteorol. Soc.* **75**, 1201 (1994)
40. <http://www.arm.gov>
41. W.G. Rees: *Physical Principles of Remote Sensing* (Cambridge University Press, Cambridge, 1990)
42. J.R. Garratt: *The Atmospheric Boundary Layer* (Cambridge University Press, 1992)
43. E.R. Westwater: *Radio Science* **13**, 677 (1978)

44. E.R. Westwater: 'Ground-based microwave remote sensing of meteorological variables', in: *Atmospheric Remote Sensing by Microwave Radiometry*, ed. by M.A. Janssen (John Wiley and Sons, New York 1993) pp. 145-213
45. J.C. Liljegren, B.M. Lesht: 'Measurements of integrated water vapor and cloud liquid water from microwave radiometers at the DOE ARM Cloud and Radiation Testbed in the U.S. Southern Great Plains', in *IEEE Int. Geosci. and Remote Sensing Symp.*, **3**, Lincoln, Nebraska, (1996) pp. 1675-1677
46. R. Friedrich, J. Peinke: *Phys. Rev. Lett.* **78**, 863 (1997)
47. B.B. Mandelbrot: *The Fractal Geometry of Nature*, (W.H. Freeman, New York, 1982)
48. D. Schertzer, S. Lovejoy: *J. Geophys. Res.* **92**, 9693 (1987)
49. P. S. Addison: *Fractals and Chaos* (Inst. of Phys., Bristol, 1997)
50. K. J. Falconer: *The Geometry of Fractal Sets* (Cambridge Univ. Press, Cambridge, 1985)
51. B. J. West, B. Deering: *The Lure of Modern Science: Fractal Thinking* (World Scient., Singapore, 1995)
52. B.B. Mandelbrot, D.E. Passoja, A.J. Paulay: *Nature* **308**, 721 (1984)
53. H. E. Hurst: *Trans. Amer. Soc. Civ. Engin.* **116**, 770 (1951)
54. H. E. Hurst, R.P. Black, Y.M. Simaika: *Long Term Storage* (Constable, London, 1965)
55. P. Flandrin: *IEEE Trans. Inform. Theory* **35**, 197 (1989)
56. M. Ausloos, N. Vandewalle, K. Ivanova: 'Time is money', in *Noise of frequencies in oscillators and dynamics of algebraic numbers*, ed. by M. Planat (Springer, Berlin, 2000) pp. 156-171
57. M. Ausloos, N. Vandewalle, Ph. Boveroux, A. Minguet, K. Ivanova: *Physica A*, **274**, 229 (1999)
58. N. Vandewalle, M. Ausloos: *Physica A* **246**, 454 (1997)
59. D.L. Turcotte: *Fractals and Chaos in Geology and Geophysics* (Cambridge University Press, Cambridge 1997).
60. M. Ausloos, K. Ivanova: *Int. J. Mod. Phys. C* **12**, 169 (2001)
61. K. Hu, Z. Chen, P.Ch. Ivanov, P. Carpena, H.E. Stanley: *Phys. Rev E* (in press) (2001).
62. R. Jullien, R. Botet: *J. Phys. A* **18**, 2279 (1985)
63. A.S. Monin, A.M. Yaglom: *Statistical Fluid Mechanics* (MIT Press, Boston 1975) Vol. 2.
64. C. Heneghan, G. McDarby: *Phys. Rev. E*, **62**, 6103 (2000)
65. U. Frisch: *Turbulence: The legacy of A.N. Kolmogorov* (Cambridge University Press, Cambridge 1995).
66. P.F. Panter: *Modulation, Noise, and Spectral Analysis* (McGraw-Hill Book Company, New York 1965)
67. M.B. Priestley: *Spectral Analysis and Time Series* (Academic Press, London 1981)
68. D.B. Percival, A.T. Walden: *Spectral Analysis for Physical Applications: Multitaper and Conventional Univariate Techniques* (Cambridge University Press, Cambridge 1994)
69. J.D. Pelletier: *Phys. Rev. Lett.* **78**, 2672 (1997)
70. N. Vandewalle, M. Ausloos: *Int. J. Comput. Anticipat. Syst.* **1**, 342 (1998)
71. A. Davis, A. Marshak, W. Wiscombe, R. Cahalan: *J. Atmos. Sci.* **53** 1538 (1996)

72. A. Marshak, A. Davis, W. Wiscombe, R. Cahalan: J. Atmos. Sci. **54**, 1423 (1997)
73. F. Schmitt, D. La Vallee, D. Schertzer, S. Lovejoy: Phys. Rev. Lett. **68**, 305 (1992)
74. Y. Tessier, S. Lovejoy, D. Schertzer: J. Appl. Meteorol. **32**, 223 (1993)
75. C. Meneveau, K.R. Sreenivasan: Phys. Rev. Lett. **59**, 1424 (1987)
76. D. La Vallee, S. Lovejoy, D. Schertzer, P. Ladoy: 'Nonlinear variability, multifractal analysis and simulation of landscape topography', in: *Fractals in Geography*. ed. by L. De Cola and N. Lam (Kluwer, Dordrecht-Boston 1993)
77. A. A. Borovkov: *Ergodicity and Stability of Stochastic Processes* (John Wiley, New York, 1998)
78. R. Holley, E.C. Waymire: Ann. J. Appl. Prob. **2**, 819 (1993)